applied sciences

MDPI

Article

A Study on the Optimization of the Louver Fin Heat Exchanger for Fuel Cell Electric Vehicle Using Genetic Algorithm

Hyeok Kwon [1], Sungyoung Park [2], Jaeho Choi [3] and Jaeyoung Han [2,*]

[1] Department of Mechanical Engineering, Kongju National University, Cheonan-si 31080, Republic of Korea
[2] Department of Future Automotive Engineering, Kongju National University, Cheonan-si 31080, Republic of Korea
[3] CAHO KOREA Co., Ltd., Asan-si 31416, Republic of Korea
* Correspondence: hjyt11@kongju.ac.kr; Tel.: +82-41-521-9241

Abstract: Fuel cell electric vehicles offer a short fuel charging time and high mileage, but require precise thermal management technology to ensure the durability and efficiency of the stack. Accordingly, the size and weight of the heat exchanger increase to ensure the performance of the heat exchanger. For this reason, a louver fin type heat exchanger requires optimal size and weight, as well as high performance. This paper optimally designs high-performance heat exchangers with reduced size and weight by applying genetic algorithms to solve this problem. The optimal result value was achieved by optimizing the design variables using concentrated variable modeling and a genetic algorithm, and the dynamic characteristics of the heat exchanger were analyzed by applying the driving cycle of the vehicle. In addition, 3D modeling was conducted to present the weight and practically applicable form. As a result, compared to the existing model, the heat transfer rate and effectiveness were improved by 5% and 1.6%, respectively, and the weight was also reduced by 5.8%. These results exceed the expected performance improvements of low size and weight. Moreover, it is expected that an improved heat exchanger optimization, as well as a design reflecting a drive cycle, could be conducted using the proposed genetic algorithm and be applied not only to a heat exchanger, but also to various components.

Keywords: genetic algorithm; heat exchanger; radiator; optimization; lumped parameter modeling; drive cycle; fuel cell vehicle

check for updates

Citation: Kwon, H.; Park, S.; Choi, J.; Han, J. A Study on the Optimization of the Louver Fin Heat Exchanger for Fuel Cell Electric Vehicle Using Genetic Algorithm. *Appl. Sci.* **2023**, *13*, 2539. https://doi.org/10.3390/app13042539

Academic Editor: Aliaksandr Shaula

Received: 20 January 2023
Revised: 7 February 2023
Accepted: 9 February 2023
Published: 16 February 2023

Copyright: © 2023 by the authors. Licensee MDPI, Basel, Switzerland. This article is an open access article distributed under the terms and conditions of the Creative Commons Attribution (CC BY) license (https://creativecommons.org/licenses/by/4.0/).

1. Introduction

Fuel cell electric vehicles (FCEVs) are expected to provide short refueling times and a long range to modern drivers [1]. Manufactures and drivers, on the other hand, have placed significant demands on technical issues including economy, stack durability, vehicle efficiency, and thermal management [2]. The quantity of heat generated by the stack increases as the vehicle's weight increases due to its high-power density. Due to the heat generated by the electrochemical reaction, maintaining high performance is exceedingly difficult and is a critical factor defining system efficiency, availability, and reliability. To solve these technical challenges, a high-performance thermal management system based on a louver fin type of compact heat exchanger (LFHX) is required [3,4]. The size and weight of the heat exchanger are particularly critical in large fuel cell vehicles. This is because the greater the drag force on the vehicle, the poorer the fuel economy and, as a result, the performance.

Many researchers have conducted various optimization studies to achieve miniaturization, high heat dissipation, and the low annual cost of the heat exchanger. To derive design parameters that satisfy single or multiple goals, optimization design techniques such as particle swarm optimization (PSO), genetic algorithm (GA), artificial bee colony algorithm (ABCA), and imperialist competitive algorithm (ICA) were typically used [5,6].

Peng et al. [7] extended the PSO method applied to the shell and tube type heat exchanger to the plate fin heat exchanger and achieved better results than the GA method by considering the total weight and annual cost of the heat exchanger as the objective function. Moreover, Zarea et al. [8] applied a hybrid type of optimization algorithm that applied a bees algorithm (BA) to PSO to a plate fin heat exchanger to improve the disadvantages of simply falling into rocker optimization or low optimization precision when the dimension of the objective function is high or local optimization exists. Hadidi et al. [9] applied ICA, which is based on human socio-political evolution, to shell and tube heat exchangers and presented its excellence through a case study. Şahin et al. [10] achieved excellence in terms of cost optimization through a case study for shell and tube heat exchangers using ABCA. GA, which is the most comparable in optimization studies, is an algorithm that mimics the natural selection process of biological evolution and is used in various types of heat exchangers. Yadav et al. [11] optimally designed an LFHX to be used in a small truck using GA and analyzed the parameters that affect heat dissipation through sensitivity analysis. Wan et al. [12] used the <second generation of nondominated sorting genetic algorithm (NSGA-II) > to derive an optimal solution through multipurpose functions of heat release and annual cost. NSGA-II is known as an algorithm that strengthens elitism and effectively maintains solution diversity through nondominated sorting and crowding distance assignment methods.

Previous studies have suggested the feasibility of heat exchanger optimization design by analyzing the effect of each design parameter, such as sensitivity analysis; however, various questions remain, and detailed formulas to confirm this and the omission of optimized key design parameter values are needed. Therefore, this paper presented geometric shape information obtained by optimizing the design information of the heat exchanger presented in Ref. [11]. In addition, the dynamic characteristics of the heat exchanger were analyzed by applying the driving cycle of the vehicle. The heat exchanger of eco-friendly hydrogen electric vehicles is still being studied because it is very important, and the optimal design study should evaluate and analyze the results within the heat management system for parts. These efforts, in addition to our research on the optimal design conditions of heat exchangers to be considered for the system unit, will improve upon the confirmation of the dynamic characteristics.

This paper is organized as follows: Section 2 describes the genetic algorithm-based optimal design technique and design information and elements for LFHX. Section 3 presents the optimal design conditions of the heat exchanger and shows the initial and final derived process. Section 4 compares and analyzes the performance characteristics of the optimized heat exchanger and applies the state of the radiator inlet side coolant derived by applying the drive cycle to the vehicle model to the heat exchanger optimization algorithm and analyzes the results.

2. Optimal Design Methodology

2.1. Lumped Parameter Modeling

Lumped parameter modeling (LPM) is a modeling technique that does not take into account the continuity of minute changes in time or space with respect to a design object's shape and design parameters. As in [13], the motor shape is optimized to quickly obtain the required power; alternatively, the geothermal reservoir and hydrogen storage tank are optimized to save costs, as in [14,15]. The lumped variable modeling used for this purpose is distinguished by increasing the calculation speed by treating each design factor, the actual dynamic characteristics of which must be reflected as a constant value and have the advantage of being simple to apply to shape and performance optimization via repetitive calculation [13–15].

However, as with finite element modeling, it does not represent changes in time and space via the continuity equation; therefore, dynamic characteristics cannot be confirmed, and only the result value is output. Furthermore, the production of a certain amount of errors, due to the assumption of a lumped variable, is regarded as a disadvantage of

the lumped parameter modeling technique. Nonetheless, the LPM can reduce the time necessary to develop an initial design model and ensure significant calculation accuracy for a design objective with low nonlinearity, such as a heat exchanger. As a result, the heat exchanger discussed in this paper is of the louvered plate fin type, and its shape characteristics and descriptions are shown in Figure 1 and Table 1.

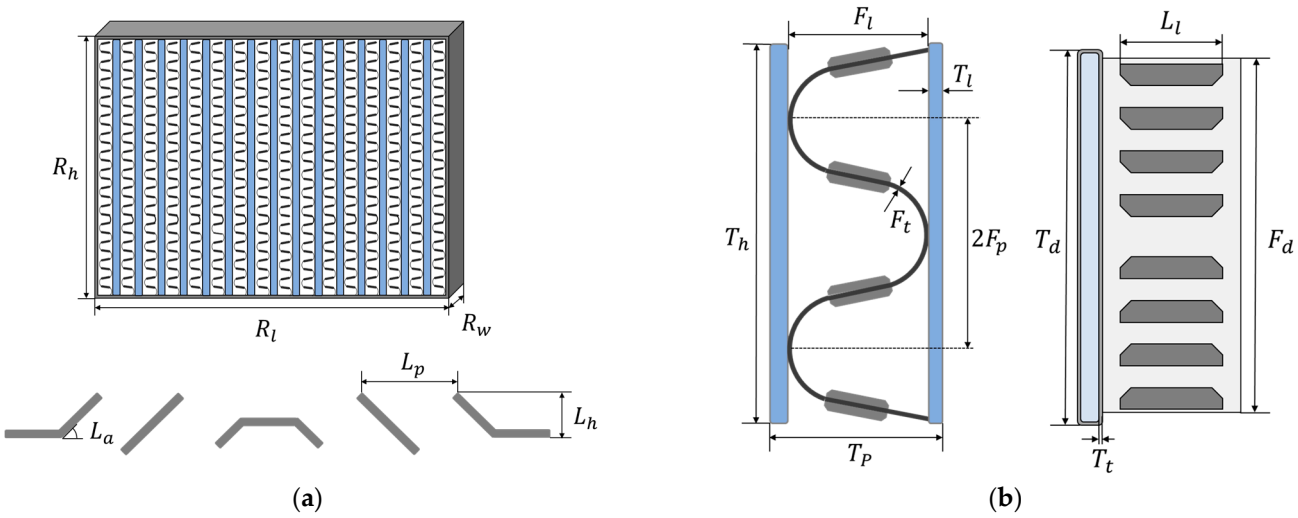

Figure 1. Geometry representation: (**a**) core and louver fin; (**b**) tube and fin.

Table 1. Nomenclature of design parameters.

Parameters	Description	Parameters	Description
A_f	Front flow area	P	Pressure
A_{ff}	Free flow area	$\dot{Q}$	Heat flow rate
C	Heat capacity	R_h	LFHX height
C_p	Specific Heat	R_l	LFHX length
ρ	Density	R_w	LFHX width
F_d	Fin depth	T_d	Tube depth
F_l	Fin length	T_h	Tube height
F_t	Fin thickness	T_l	Tube length
F_p	Fin pitch	T_P	Tube pitch
$\dot{m}$	Mas flow rate	T_t	Tube thickness
L_a	Louver angle	N_T	Number of tubes
L_h	Louver height	N_f	Number of fins
L_l	Louver length	NTU	Number of transfer unit
L_p	Louver pitch	T	Temperature
RW	Total weight	ε	Effectiveness
$efin$	Fin efficiency		

2.2. Genetic Algorithm

Genetic algorithm (GA) are widely used in the field of optimization design as a method that mimics the natural selection process of biological evolution. Utilizing this, GA can be used to improve the efficiency of centrifugal compressor impellers [16], optimize motor design [17], identify lithium-ion battery parameters, and validate data [18].

Therefore, the flowchart of the genetic algorithm is shown in Figure 2, and the operating method can be summarized in five steps as follows.

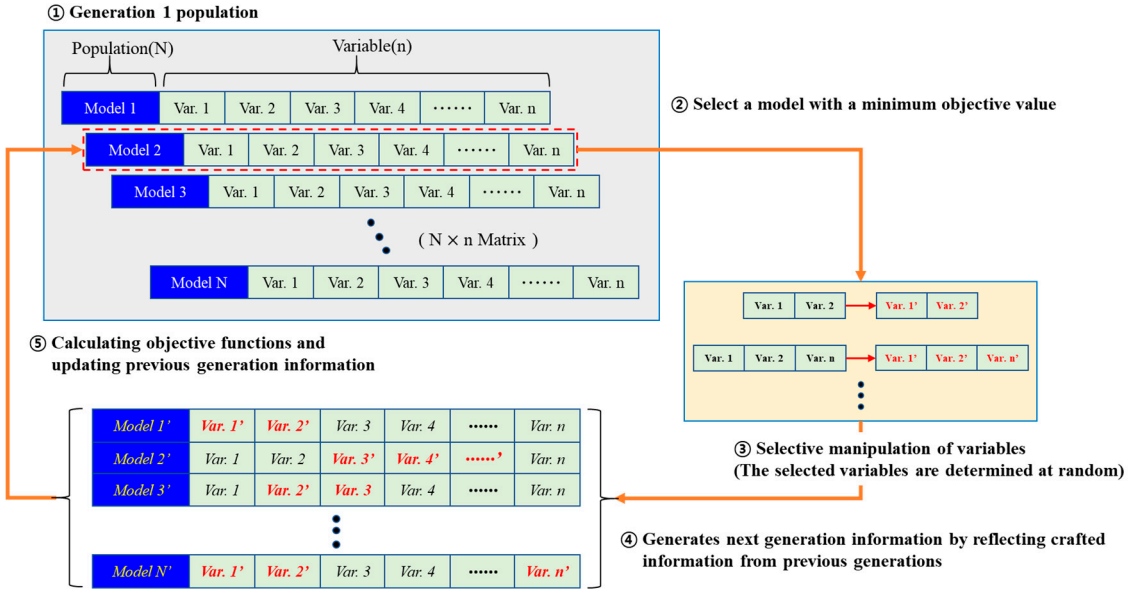

Figure 2. Flowchart of genetic algorithm.

(1) Initialization: Creation of the first-generation population;

(2) Selection: Choose a model from the smallest objective function value among the population, and the model is defined as the initial model before optimization;

(3) Mutation: The variables of the initial model are randomly chosen, and the values of the selected variables are mutated. At this moment, the number of variables selected is randomly determined, and, on average, around 50% of all shape variables are selected for variation;

(4) Crossover: Create a population with a new value in the next generation based on information from the previous generation;

(5) Replace: When a model with a lower objective function value compared to the optimal model of the previous generation is observed among the models of the next generation population, the value of the current generation evaluated as the objective function is selected from the variable information of the previous generation.

2.3. Governing Equation

The LFHX is one of the heat exchangers in charge of heat exchange in the cooling system and is a thermal management component that cools the temperature of the coolant through heat exchange with outside air to control the vehicle temperature. The LFHX must be used by selecting the type of heat exchanger that is designed to meet the heat transfer requirements within the constraints. It was intended to measure the outlet temperature utilizing the coolant, air flow rate, and inlet temperature as parameters based on the heat exchange theory, the effectiveness-NTU method, in order to correctly understand the heat exchange characteristics. When the type and dimensions of the heat exchanger are specified, the effectiveness-NTU method calculates the heat transfer and outlet temperature for a particular mass flow rate and inlet temperature. In other words, it is used when the heat transfer area is known and the outlet temperature needs to be derived, and the heat transfer performance of a specified heat exchanger needs to be determined, or whether the heat exchanger can work. Effectiveness is defined as the ratio of the actual heat transfer rate/maximum possible heat transfer rate and is based on a dimensionless coefficient called heat transfer effectiveness. The heat exchange characteristics of the LFHX can be determined by calculating the effectiveness 'ε' based on the flow rate and temperature of the cooling water and outside air. Figure 3 is a flowchart of the procedure for obtaining the heat transfer rate, which is one of the performance indicators of the heat exchanger, and the heat transfer rate is finally obtained using the effectiveness-NTU method. In this study,

the temperature of the cooling water is determined according to the temperature of the outside air by using the effectiveness-NTU method based on the geometry of the louver fin, and the pressure is calculated by taking into account the pressure drop and head loss in the LFHX inner tube.

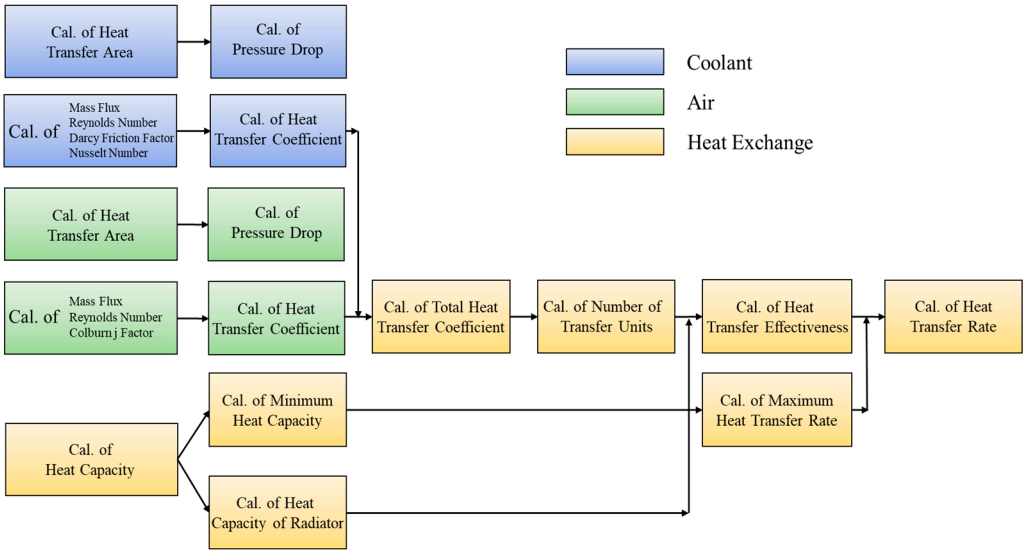

Figure 3. Calculation flowchart of performance for heat exchanger.

The heat transfer coefficient of the cooling water (h_w) can be calculated as in the following equation [19,20]:

$$h_w = \frac{N_u \times k_w}{D_h} \tag{1}$$

$$N_u = 0.332 {Re_w}^{0.5} {Pr_w}^{0.333} \tag{2}$$

$$D_{hw} = \frac{2(T_l \times 2T_t)(T_d - 2T_t)}{(T_l + T_d - 2T_t)} \tag{3}$$

$$Re_w = \frac{(\dot{m} \times D_{hw})}{\mu_w \{2(T_l \times 2T_t)(T_d - 2T_t) N_T\}} \tag{4}$$

where N_u, D_{hw}, and Re_w are the Nusselt number, hydraulic diameter, and Reynolds number of the coolant, respectively.

The heat transfer coefficient of air (h_a) is calculated as

$$h_a = j\ G\ C_{pa}\ Pr^{-2/3} \tag{5}$$

The Colburn factor (j) is given by [21]

$$j = \begin{pmatrix} Re_{air}^{-0.49} & \times \left(\frac{L_a}{90}\right)^{0.27} \times \left(\frac{Fp}{Lp}\right)^{-0.14} \times \left(\frac{Fl}{Lp}\right)^{-0.29} \times \left(\frac{T_d}{Lp}\right)^{-0.23} \\ & \times \left(\frac{Ll}{Lp}\right)^{0.68} \times \left(\frac{Fl+T_h}{Lp}\right)^{-0.28} \times \left(\frac{F_t}{Lp}\right)^{-0.05} \end{pmatrix} \tag{6}$$

In this case, L_a is defined in the range between 15° and 30°, which implies that, as the angle of the louver pin increases, the heat transfer area increases and the air flows between the louvers in the low Reynolds number region; thus, the angle must be appropriately increased. However, in the high Reynolds number region, air flows between the louvers even if the angle is small; therefore, it must be chosen appropriately, considering the friction coefficient and pressure drop according to the increase in angle [22–24].

The Prandtl number of air (Pr) is given by

$$Pr = \frac{C_{pa}\,\mu_a}{k_a} \tag{7}$$

where C_{pa}, μ_a, and k_a are the specific heat capacity, dynamic viscosity, and thermal conductivity of air, respectively.

The hydraulic diameter of air (D_{ha}) is given by [11]

$$D_{ha} = \frac{2\{(F_p - F_t) \times F_l\}}{\{(F_p - F_t) + F_l\}} \tag{8}$$

The air mass flux (G) is given by

$$G = \rho_a \times V_a \tag{9}$$

where ρ_a and V_a are the air density and velocity, respectively.

Calculation of heat transfer rate ($\dot{Q}$) is given by

$$\dot{Q} = \varepsilon \times Q_{max} \tag{10}$$

$$Q_{max} = \frac{C_{min}}{(T_{w,in} - T_{a,in})} \tag{11}$$

$$\varepsilon = 1 - exp\left\{\frac{NTU^{0.22}}{C_r}\left[\exp\left(-C_r \times NTU^{0.78}\right) - 1\right]\right\} \tag{12}$$

$$NTU = \frac{1}{\left(\frac{1}{h_w A_w}\right) + R_{th} + \left(\frac{1}{h_a A_a}\right)} \tag{13}$$

$$C_r = \frac{C_{min}}{C_{max}} \tag{14}$$

where Q_{max} and ε are the maximum heat transfer rate and the heat transfer effectiveness. Moreover, NTU and C_r are the number of transfer units and the heat capacity ratio.

The minimum heat capacity rate (C_{min}) is a small one between C_w and C_a, where C_w and C_a are the heat capacity rate of the coolant and air, respectively, and are obtained as follows.

$$C_w = \dot{m}_w \times C_{pw} \tag{15}$$

$$C_a = \dot{m}_a \times C_{pa} \tag{16}$$

A_w is the cooling water side heat transfer area and is given as follows [25].

$$A_w = N_t\{(2T_h \times T_d) + (2T_h \times T_l)\} \tag{17}$$

A_a is the air side heat transfer area and is given as follows.

$$A_a = \left(A_f - A_{ff}\right) \times (N_t + 1) \tag{18}$$

$$A_f = F_l \times T_h \tag{19}$$

$$A_{ff} = F_l \times T_h - \{F_t \times (F_l - L_l) + L_l \times L_h\} \times N_f \tag{20}$$

R_{th} is the contamination factor and is given as [11]:

$$R_{th} = \left(\frac{1}{2pi \times k_{al} \times T_l}\right) \times log\left(\frac{D_o}{D_o - 2N_T}\right) \tag{21}$$

Here, k_{al} is the thermal conductivity of the aluminum alloy and is 150 [W/m^2·K].

D_o is the equivalent diameter, given by [11]

$$D_o = \frac{(T_d \times T_l)^{0.625}}{\left\{\sqrt{\left(\frac{T_d^2}{2}\right) + \left(\frac{T_l^2}{2}\right)}\right\}^{0.25}} \tag{22}$$

The pressure-drop of the cooling water (d_{Pw}) is obtained as follows.

$$d_{Pw} = f_w \times \frac{T_h}{D_{hw}} \times \frac{\rho_w {V_w}^2}{2} \tag{23}$$

where ρ_w and V_w are the coolant density and velocity, respectively.

The friction coefficient (f_w) on the coolant side is given as [26]:

$$\begin{aligned} f_w &= 64/Re_w \quad \text{(Laminar flow)} \\ f_w &= (0.790\ ln\ Re - 1.64)^{-2} \quad \text{(Turbulent flow)} \end{aligned} \tag{24}$$

The air pressure-drop of air (d_{Pa}) is obtained as:

$$d_{Pa} = f_a \left(\frac{A_a}{A_w}\right) \frac{\rho_a {V_a}^2}{2} \tag{25}$$

The air side friction coefficient (f_a) is given by [27]

$$f_a = 0.54486 {Re_a}^{-0.3068} \left(\frac{L_a}{90}\right)^{0.444} \left(\frac{Fp}{Lp}\right)^{-0.9925} \left(\frac{Fl}{Lp}\right)^{0.5458} \left(\frac{L_h}{Lp}\right)^{-0.2003} \left(\frac{F_d}{Lp}\right)^{0.0688} \tag{26}$$

3. Analysis with Optimization Process

In this paper, the optimization design for the LFHX for a small truck presented in [11] was re-executed through the optimal design process shown in Figure 4, and the current optimal design results obtained were compared and analyzed based on the performance calculated with the optimal design parameters presented in [11].

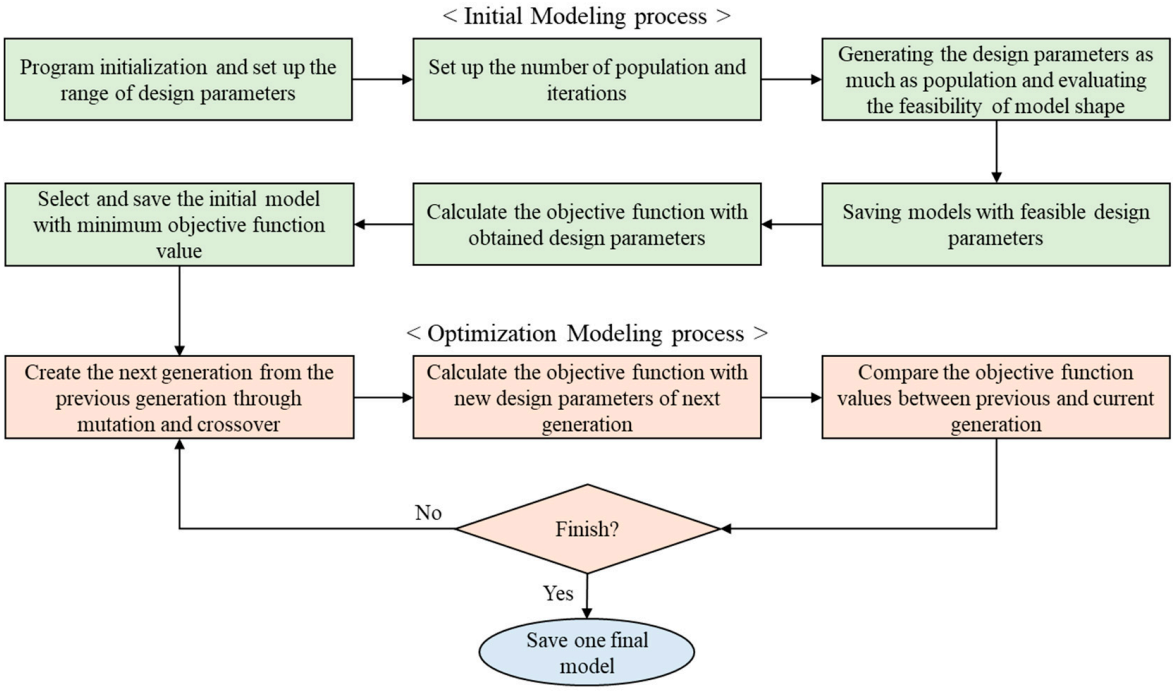

Figure 4. Optimal design process for initial and final models.

Initial Condition

Prior to optimization, the physical properties and operating conditions of air and coolant in [11] were defined identically as shown in Tables 2 and 3, and the types and ranges of heat exchanger design parameters were revised as shown in Table 4. Furthermore, the number of optimization iterations was set to 1 million, and the number of populations was set to 250. The criteria for stopping genetic algorithms are when 98% of the population set has the same shape determinant and the objective function value becomes the same, or when the number of iterations reaches the number of iterations set by the user.

Table 2. Air and coolant properties.

	Properties	Values
Air	Density (ρ_a)	1.165 kg/m^3
	Dynamic viscosity (μ_a)	18.63×10^{-6} Ns/m^2
	Specific heat capacity (C_{pa})	1005 J/kg K
	Thermal conductivity (k_a)	0.02675 W/m K
Coolant	Density (ρ_w)	980 kg/m^3
	Dynamic viscosity (μ_w)	0.3344×10^{-3} Ns/m^2
	Specific heat capacity (C_{pw})	4188 J/kg K
	Thermal conductivity (k_w)	0.656 W/m K
	Prandtl number (Pr)	2.85

Table 3. Operating conditions.

Properties	Values
Air Temperature (T_a)	28 [°C]
Air Pressure (P_a)	101.325 [kPa]
Air Velocity (V_a)	14 [m/s]
Coolant Temperature (T_w)	80 [°C]
Coolant Pressure (P_w)	101.325 [kPa]
Coolant Mass flow rate ($\dot{m}_w$)	0.1671 [kg/s]

Table 4. Dimension ranges for LFHX.

Design Parameters	Min.	Max.
R_l [mm]	0.3	0.4
T_l [mm]	0.001	0.003
T_h [mm]	0.25	0.3
T_d [mm]	0.0156	0.0254
N_t	30	50
F_r [mm]	0.0005	0.002
ratL_l	0.8	0.95
ratF_d	0.9	1.1
N_f	150	300
L_h [mm]	0.0001	0.002
L_p [mm]	0.0001	0.002

Regarding optimization using GA, the result varies depending on the objective function setting, and the main performance indicators are set according to the designer's intention and are reflected in the objective function. In this paper, heat transfer rate (A), effectiveness (B), fin efficiency (C), and total weight (D) of the heat exchanger were set as main indicators, and the basic formula is as follows.

$$Objective\ Function = \sqrt{k_1A^2 + k_2B^2 + k_3C^2 + k_4D^2}\ ,\ k_1 + k_2 + k_3 + k_4 = 1 \quad (27)$$

In the above formula, k represents the weight of each term and, in this paper, it is set to 0.4, 0.3, 0.2, and 0.1 in order, respectively. Moreover, the optimization proceeds in the direction which minimizes the value of the objective function.

4. Results and Discussion

Optimization using GA took about 2 h while running a total of 33,208 iterations. Each result value calculated with the optimization design parameters is presented in [11] and the results of the model optimized in this paper are shown in Table 5. The detailed shape of the optimized LFHX is shown in Figure 5.

Table 5. The results of the reference model, initial model, and optimized model.

Parameters	Ref. [11]	Initial Model	Final Model
R_l [mm]	359.854	340.929	359.854
R_h [mm]	285.532	274.197	285.002
R_w [mm]	19.027	18.5002	17.124
RW [kg]	0.863	0.782	0.813
$\dot{Q}$ [kW]	25.008	20.859	26.262
ε	0.912	0.952	0.928
$efin$	0.789	0.816	0.779

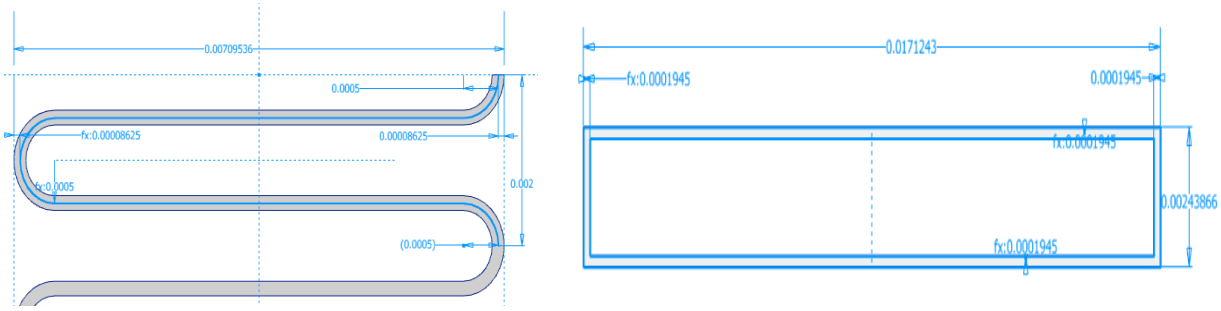

(**a**) (**b**)

Figure 5. Three-dimensional modeling of heat exchanger: (**a**) sketch and parameters at fin front view; (**b**) sketch and parameters at plane view.

As shown in Table 5, the heat transfer rate of the starting model produced from the optimization process is lower than the comparable value of the reference model, while the heat transfer rate of the final model after optimization is increased by about 5% compared to the reference model. Furthermore, effectiveness increased by about 1.6%, and overall weight decreased by about 5.8%; however, fin efficiency decreased by 1%. As a result, it is expected that the heat dissipation performance can be improved by roughly 5% by considering effectiveness and fin efficiency, which were not included in Ref. [11].

Because the current heat exchanger is optimized and based on one specific operating point of the vehicle, it is necessary to investigate performance variations over the whole driving range of the vehicle. Changes in the mass flow rate, temperature, and pressure of coolant and air, which are the heat exchanger's input boundary conditions, affect the heat transfer rate, effectiveness, and pressure drop, and may cause changes in design parameters to satisfy the required performance during the optimization process.

4.1. Driving Cycle

A drive cycle is a time-based value that is used to expresses and assess vehicle operating parameters such as torque, fuel economy, ram air, and cooling performance. It was used as an input value of a vehicle model in this study to evaluate the performance of a lightweight vehicle LFHX and was simulated under two conditions: Highway Fuel Driving Schedule (HWFET) and Urban Dynamometer Driving Schedule (UDDS), both of which were developed by the US Environmental Protection Agency (EPA).

As shown in Figure 6a, the HWFET travels 16.45 km at an average speed of 77.7 km/h for 765 s and is used to express high-speed driving conditions. It was used to confirm the characteristics of the cooling system under continuous vehicle load conditions. As

shown in Figure 6b, UDDS travels 12 km at an average speed of 32 km/h for 1369 s and is used to depict city driving conditions. It was used to test actual vehicle characteristics in urban driving conditions; deceleration, stop, and acceleration are frequent performances according to traffic conditions in an urban environment.

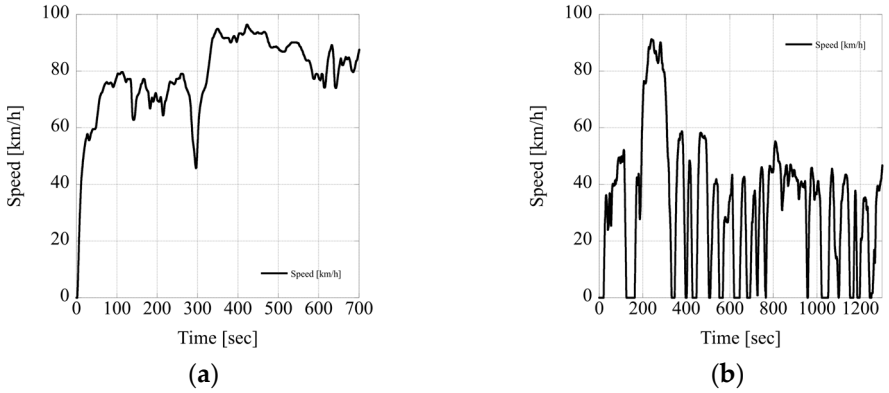

Figure 6. (**a**) High-speed driving conditions in the driving cycle; (**b**) urban driving conditions in the driving cycle.

Figure 7 shows an integrated thermal management system model for electric battery vehicles. The purpose of this model is to derive the heat value of the powertrain unit according to vehicle driving conditions and state, and to cool it to properly maintain the operating temperature of each unit, while satisfying the cabin heating and cooling performance desired by the passenger. The orange line flow path, which uses a 50:50 mixture of water and ethylene glycol as the working fluid, operates in two methods, series and parallel, via the four-way valve. If operating in series, the four-way valves are connected according to A–D and B–C. In this case, the radiator is responsible for cooling the charger, motor, and inverter, and the battery and DC–DC converter are handled by the chiller. When the operation is performed in the parallel manner, the operation is connected according to A–B and C–D. In this case, the cooling of all powertrain units is performed through an integrated cooling flow path.

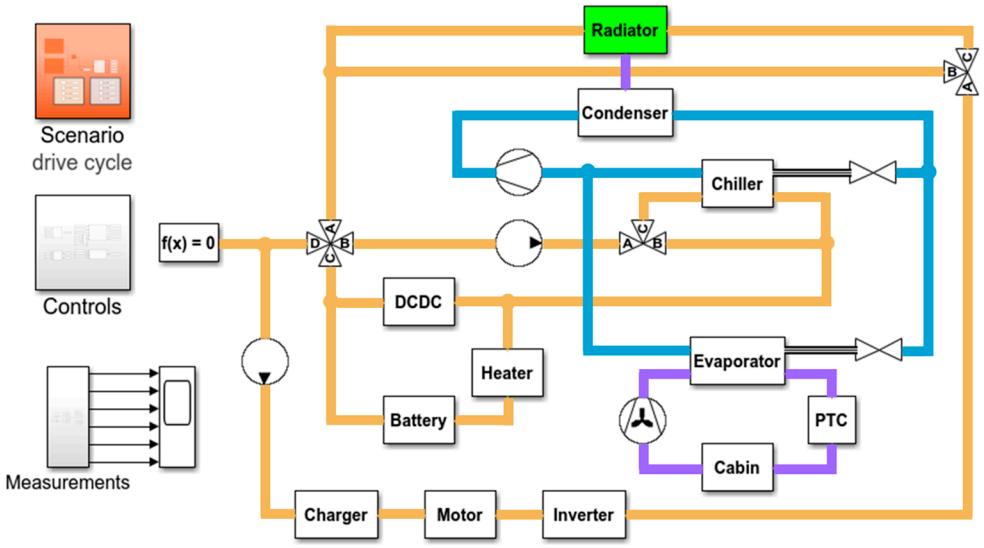

Figure 7. Electric vehicle model used in MATLAB (Simscape).

4.2. Dynamic Performances

In this paper, the inlet condition of the heat exchanger which was extracted using each driving cycle shown in Figure 6 was added to Figure 7, and the performance was calculated using the shape information of the optimization model. Figures 8 and 9, show the input

condition of the heat exchanger to verify the dynamics, which is extracted using the process shown in Figure 6. Here, a total of five performance indicators are measured, namely, heat transfer rate, effectiveness, fin efficiency, air side pressure drop, and coolant side pressure drop, respectively, and the results are presented in Figures 10 and 11.

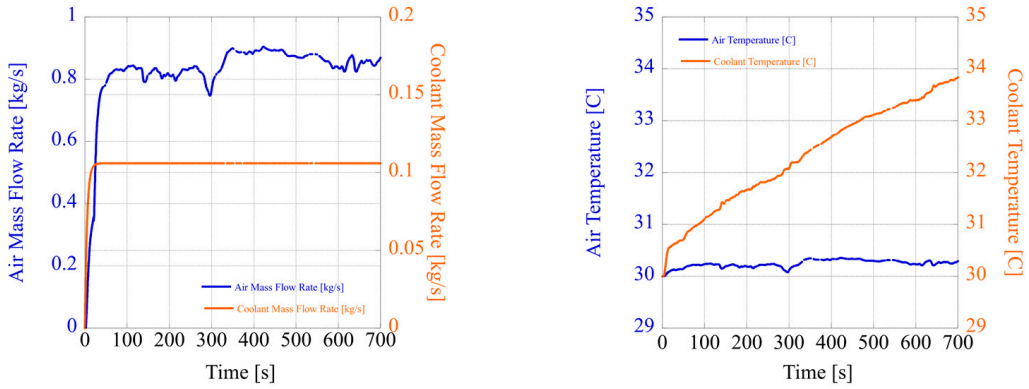

(**a**) (**b**)

Figure 8. Inlet boundary condition in HWFET: (**a**) mass flow rate in air side and coolant side; (**b**) temperature in air side and coolant side.

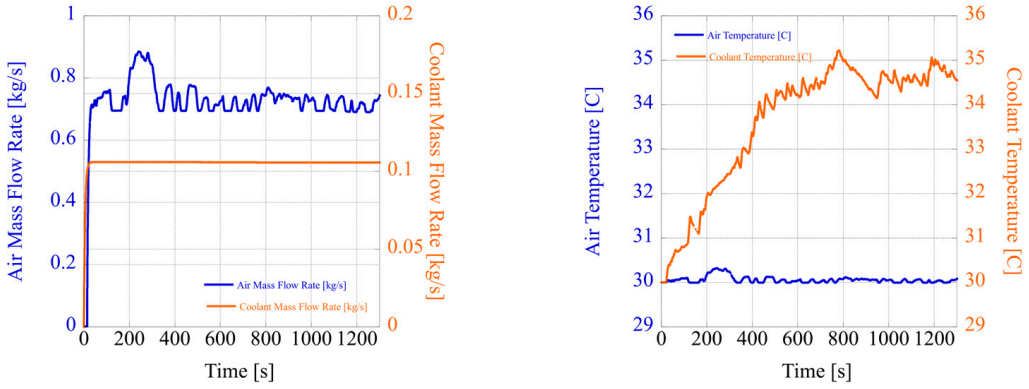

(**a**) (**b**)

Figure 9. Inlet boundary condition in UDDS: (**a**) mass flow rate in air side and coolant side; (**b**) temperature in air side and coolant side.

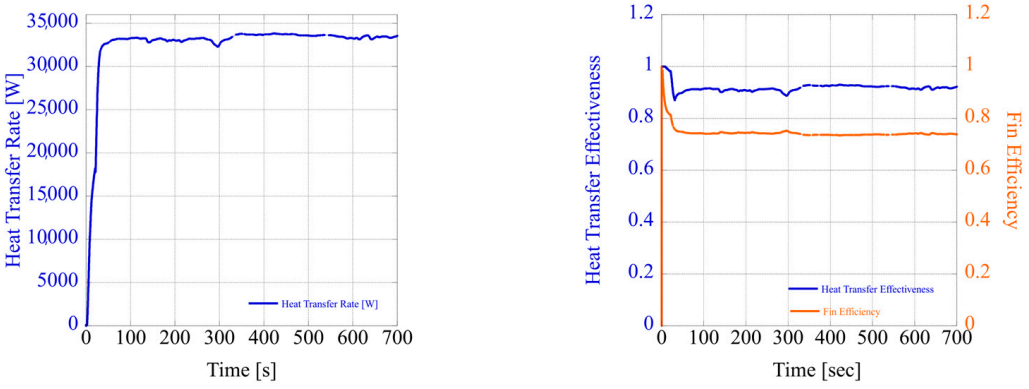

(**a**) (**b**)

Figure 10. Optimal design heat exchanger results at HWFET Drive cycle: (**a**) Heat transfer rate; (**b**) Heat exchanger Effectiveness and Fin efficiency.

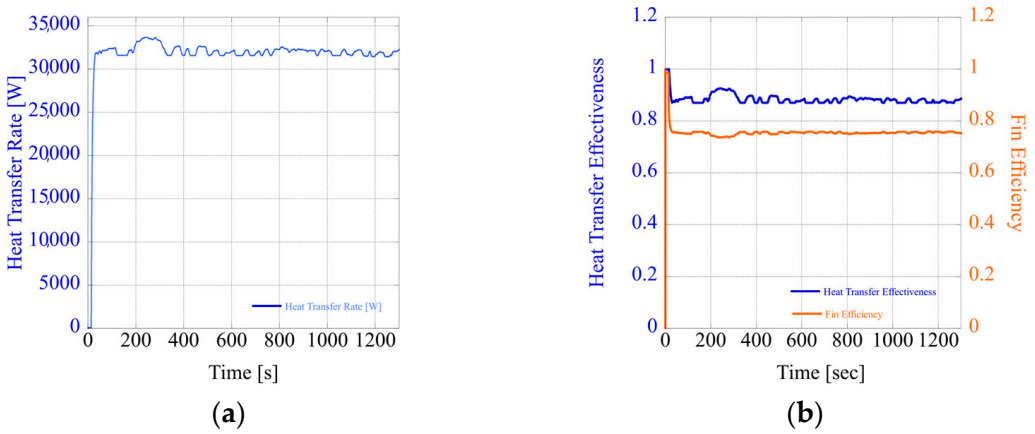

Figure 11. Optimal design heat exchanger results at UDDS drive cycle: (**a**) heat transfer rate; (**b**) heat exchanger effectiveness and fin efficiency.

4.2.1. HWFET

The heat transfer rate and its effectiveness showed comparable trends as a consequence of the performance calculation; however, fin efficiency showed contrary trends. In addition, the pressure drop in the air side shows a similar trend to the mass flow rate of air in Figure 8a. Moreover, as shown in Figure 8a, because there was no change in the coolant mass flow rate, the pressure drop on the coolant side was found to be minimal. Other than the air side pressure drop in the HWFET scenario, the overall performance difference is minor.

4.2.2. UDDS

As mentioned in Section 4.2.1, the behavior of each performance indicator shows a similar trend even under the UDDS condition. However, comparing the average values of effectiveness and fin efficiency according to the driving conditions in Figures 10 and 11 shows 0.924/0.765 and 0.887/0.768, respectively. The effectiveness of HWFET is slightly higher than that of UDDS; however, fin efficiency shows the opposite result.

If it is possible to secure the driving cycle according to the type of eco-friendly vehicle, it is expected to be able to apply the optimal heat exchanger design through dynamic performance analysis. This would be useful, for example, to optimize the heat transfer rate, effectiveness, fin efficiency, and the total weight of a vehicle that maintains a low or high driving load state for a long time; moreover, it will be possible to perform an optimal design considering multiple operating points for each vehicle. At this time, it is thought that research is needed to properly set the items and their respective weights to be reflected in the objective function.

5. Conclusions

To optimize the compact heat exchanger design required for eco-friendly vehicles, in this paper, a GA-based heat exchanger optimization design program with objective functions of heat transfer rate, effectiveness, fin efficiency, and total weight was developed. The design parameter optimization was conducted through about 33,000 iterations; moreover, 250 populations were created, and the objective function value converged to a certain level. The process and results are as follows.

(1) An optimal design was performed for a commonly used LFHX;

(2) For comparison with the existing optimization model, the design parameter setting range of the heat exchanger was set to be larger than that of the existing model;

(3) As a result of the optimization, the final model improved the heat transfer rate, effectiveness, and total weight by 5%, 1.6%, and 5.8%, respectively, compared to the design reference model in [11]; however, the fin efficiency decreased by 1%.

In the above results, we re-optimized the already optimized models; therefore, although performance improvements may not be significant, they have been reduced in size and weight, making them smaller.

In addition, to confirm the dynamic characteristics of the heat exchanger designed at a specific single operating point, HWFET for highway driving conditions and UDDS for city driving conditions were applied to the MATLAB® (Simscape) vehicle model to extract the heat exchanger inlet boundary conditions. As a result of applying the corresponding input data to the optimized final model, it was confirmed that the heat transfer rate, effectiveness, and fin efficiency among the performance indicators of the heat exchanger changed as the driving load condition of the vehicle changed. This result means that it is possible to optimize the heat exchanger design based on the performance at multiple operating points; thus, it is expected that it will be possible to design a heat exchanger with improved average performance rather than a heat exchanger using a single operating point.

The optimization design program developed using the genetic algorithm has the advantage of being universally used for the optimal design of various types of heat exchangers used in eco-friendly vehicles. It can be said that the utilization value of this study is high because it can be expanded and applied to fields relating to the optimal design of other element parts, including heat exchangers, that do not have large nonlinearity.

Author Contributions: H.K. designed and applied the proposed optimization technique. Literature reviews, formula analysis, and simulations were carried out by H.K. and S.P.; The shape review and result derivation of the simulation results were carried out by H.K. and J.C.; Final review of manuscript corrections was done by J.H. All authors have read and agreed to the published version of the manuscript.

Funding: This result was supported by "Regional Innovation Strategy (RIS)" through the National Research Foundation of Korea (NRF) funded by the Ministry of Education (MOE) (2021RIS-004).

Institutional Review Board Statement: Not applicable.

Informed Consent Statement: Not applicable.

Data Availability Statement: Not applicable.

Conflicts of Interest: The authors declare no conflict of interest.

References

1. Emadi, A.; Williamson, S.S. Fuel Cell Vehicles: Opportunities and Challenges. In Proceedings of the IEEE Power Engineering Society General Meeting 2004, Denver, CO, USA, 6–10 June 2004; pp. 1640–1645.
2. Rajashekara, K. Power Conversion and Control Strategies for Fuel Cell Vehicles. In Proceedings of the IECON'03, 29th Annual Conference of the IEEE Industrial Electronics Society (IEEE Cat. No. 03CH37468), Roanoke, VA, USA, 2–6 November 2003; Volume 3, pp. 2865–2870.
3. Gong, C.; Shen, J.; Yu, Y.; Wang, K.; Tu, Z. A Novel Radiator Structure for Enhanced Heat Transfer Used in PEM Fuel Cell Vehicle. *Int. J. Heat Mass Transf.* **2020**, *157*, 119926. [CrossRef]
4. Jang, J.-Y.; Chen, C.-C. Optimization of Louvered-Fin Heat Exchanger with Variable Louver Angles. *Appl. Therm. Eng.* **2015**, *91*, 138–150. [CrossRef]
5. Kao, Y.-T.; Zahara, E. A Hybrid Genetic Algorithm and Particle Swarm Optimization for Multimodal Functions. *Appl. Soft Comput.* **2008**, *8*, 849–857. [CrossRef]
6. Osmani, A.; Mohasefi, J.B.; Gharehchopogh, F.S. Sentiment Classification Using Two Effective Optimization Methods Derived from The Artificial Bee Colony Optimization and Imperialist Competitive Algorithm. *Comput. J.* **2022**, *65*, 18–66. [CrossRef]
7. Peng, H.; Ling, X.; Wu, E. An Improved Particle Swarm Algorithm for Optimal Design of Plate-Fin Heat Exchangers. *Ind. Eng. Chem. Res.* **2010**, *49*, 6144–6149. [CrossRef]
8. Zarea, H.; Kashkooli, F.M.; Soltani, M.; Rezaeian, M. A Novel Single and Multi-Objective Optimization Approach Based on Bees Algorithm Hybrid with Particle Swarm Optimization (BAHPSO): Application to Thermal-Economic Design of Plate Fin Heat Exchangers. *Int. J. Therm. Sci.* **2018**, *129*, 552–564. [CrossRef]
9. Hadidi, A.; Hadidi, M.; Nazari, A. A New Design Approach for Shell-and-Tube Heat Exchangers Using Imperialist Competitive Algorithm (ICA) from Economic Point of View. *Energy Convers. Manag.* **2013**, *67*, 66–74. [CrossRef]
10. Şahin, A.S.; Kılıç, B.; Kılıç, U. Design and Economic Optimization of Shell and Tube Heat Exchangers Using Artificial Bee Colony (ABC) Algorithm. *Energy Convers. Manag.* **2011**, *52*, 3356–3362. [CrossRef]

11. Yadav, M.S.; Giri, S.A.; Momale, V.C. Sizing Analysis of Louvered Fin Flat Tube Compact Heat Exchanger by Genetic Algorithm. *Appl. Therm. Eng.* **2017**, *125*, 1426–1436. [CrossRef]
12. Wan, R.; Liu, Z.; Wu, H.; Cheng, Q.; Ding, H. Modeling and Performance Optimization of Louvered Fin Radiators in Negative Gauge Pressure Condition. *Adv. Theory Simul.* **2022**, *5*, 2100463. [CrossRef]
13. Lovelace, E.C.; Jahns, T.M.; Lang, J.H. A Saturating Lumped-Parameter Model for an Interior PM Synchronous Machine. *IEEE Trans. Ind. Appl.* **2002**, *38*, 645–650. [CrossRef]
14. Axelsson, G.; Björnsson, G.; Quijano, J.E. Reliability of Lumped Parameter Modeling of Pressure Changes in Geothermal Reservoirs. In Proceedings of the World Geothermal Congress, Melbourne, Australia, 19–25 April 2005; pp. 1–8.
15. Wang, C.-S.; Brinkerhoff, J. Low-Cost Lumped Parameter Modelling of Hydrogen Storage in Solid-State Materials. *Energy Convers. Manag.* **2022**, *251*, 115005. [CrossRef]
16. Li, X.; Liu, Z.; Lin, Y. Multipoint and Multiobjective Optimization of a Centrifugal Compressor Impeller Based on Genetic Algorithm. *Math. Probl. Eng.* **2017**, *2017*, e6263274. [CrossRef]
17. Hyun, D.; Yun, D.; Baek, J. Optimal Design of a Six-Phase Permanent-Magnet-Assisted Synchronous Reluctance Motor to Convert into Three Phases for Fault-Tolerant Improvement in a Traction System. *Appl. Sci.* **2021**, *11*, 8508. [CrossRef]
18. Zhang, L.; Wang, L.; Hinds, G.; Lyu, C.; Zheng, J.; Li, J. Multi-Objective Optimization of Lithium-Ion Battery Model Using Genetic Algorithm Approach. *J. Power Sources* **2014**, *270*, 367–378. [CrossRef]
19. Lee, S.H.; Kim, M.; Ha, M.Y.; Park, S.-H.; Min, J.K. Heat Exchanger Ranking Program Using Genetic Algorithm and ε-NTU Method for Optimal Design. *Trans. Korean Soc. Mech. Eng. B* **2014**, *38*, 925–933. [CrossRef]
20. Sanaye, S.; Hajabdollahi, H. Thermal-Economic Multi-Objective Optimization of Plate Fin Heat Exchanger Using Genetic Algorithm. *Appl. Energy* **2010**, *87*, 1893–1902. [CrossRef]
21. Asadi, M.; Nadali, A. Study on the Functions of Friction and Colburn Factors in Compact Heat Exchanger. *Wyno Acad. J. Eng. Technol. Res.* **2013**, *1*, 37–48.
22. Oh, Y.M.; Su-Ryong, L. A 3D Numerical Study on the Performance of Automotive Louvered Fin Heat Exchanger for Different Louver Angles. *J. Korean Soc. Mech. Technol.* **2017**, *19*, 235–241. [CrossRef]
23. Jiin-Yuh, J.; Ying-Chi, T. Optimum Louver Angle Design for a Louvered Fin Heat Exchanger. *Int. J. Phys. Sci.* **2011**, *6*, 6422–6438. [CrossRef]
24. Gunnasegaran, P.; Shuaib, N.H.; Abdul Jalal, M.F. The Effect of Geometrical Parameters on Heat Transfer Characteristics of Compact Heat Exchanger with Louvered Fins. *Int. Sch. Res. Not.* **2012**, *37*, 1078–1086. [CrossRef]
25. Shah, R.K.; Sekulic, D.P. *Fundamentals of Heat Exchanger Design*; John and Wiley and Sons: Hoboken, NJ, USA, 2003.
26. Yunus, C.; Ghajar, A. *Heat and Mass Transfer Fundamentals and Applications*, 6th ed.; McGraw Hill: New York, NY, USA, 2019; p. 992.
27. Dong, J.; Chen, J.; Chen, Z.; Zhang, W.; Zhou, Y. Heat Transfer and Pressure Drop Correlations for the Multi-Louvered Fin Compact Heat Exchangers. *Energy Convers. Manag.* **2007**, *48*, 1506–1515. [CrossRef]

Disclaimer/Publisher's Note: The statements, opinions and data contained in all publications are solely those of the individual author(s) and contributor(s) and not of MDPI and/or the editor(s). MDPI and/or the editor(s) disclaim responsibility for any injury to people or property resulting from any ideas, methods, instructions or products referred to in the content.